24th COBEM - 2017

24th ABCM International Congress of Mechanical Engineering
December 3-8, 2017, Curitiba, PR, Brazil

COBEM-2017-0745
NUMERICAL STUDY ON THE PERFORMANCE OF SQUARE TUBES AS ENERGY ABSORBERS

José Carlos de Souza Teles
Rita de Cássia Silva
Alessandro Borges de Sousa Oliveira
University of Brasília, Brasília DF, Brazil
jdeteles@hotmail.com, ritasilva@unb.br, abso@unb.br

Abstract. *This work consists in a numerical study on the performance of square tubes under quasi-static progressive buckling, where strain rate and inertial forces are not considered. Such shell structures have been applied in vehicles as passive safety device. In fact, they may reduce or avoid passengers to suffer severe or fatal injuries in case of frontal crashes. In this context, simulations using FEM (Finite Element Method) are performed to evaluate the behaviour of such structures loaded under axial crushing. For this, some parameters such as tube wall thickness and type of material are assessed in the performance of the energy absorbers during a crushing process. The energy absorbed is calculated using the load-displacement curve obtained from simulations and comparisons among these values are done in order to verify the influence of the changes in the parameters studied. In this work, the effect of changes in wall thickness and material properties are studied by analysing the variation in the energy absorbed, specific energy absorption, load peak, and mean crushing load, which are crashworthiness parameters explained in section 1. The results showed that all crashworthiness parameters considered varies when the wall thickness and material properties are changed. Also, variations on the collapsible profile of the specimens were observed.*

Keywords: *crushing, energy absorbers, crash box.*

1. INTRODUCTION

Nowadays automobiles are a widely mode of transportation used by society. Actions related to safety are necessary to prevent or minimize harm in vehicle occupants. In this sense, the study on how automotive structures crush is necessary since their plastic deformation absorbs the kinetic energy during car collisions. Such studies can be performed by experimental studies, numerical simulations and by analytical predictions obtained in the literature. One structure widely studied due its role in energy absorption in car crashes is called crash box. This device is an energy absorber and is usually placed between the bumper and the vehicle side members. A crash box absorbs a large percentage of the kinetic energy during the collision by its deformation, which decreases the acceleration felt by car occupants.

Many authors have studied the performance of tubes as energy absorbers. Their works include both numerical simulations and experimental analysis. The methodology used by these authors consists in perform compression tests in specimens in order to obtain the energy absorbed and the mean crushing force. Most of them compare the results obtained with the analytical predictions available in the literature. A few examples of such studies are briefly described in this section.

In all cases studied in the present work, the load-displacement curve of the crushing process is obtained and analysed. This curve was explained by Paik, *et al*.; 1996 and is presented in Fig. 1. According to these authors, the axial force will rapidly drop after the ultimate load (P_u) is reached. As the deformation continues, the walls will fold until they contact each other. After this contact occurs, the force rises again until the adjacent walls fold. This behaviour repeats until the folding of the walls ends. The completely folded structures behaves as a rigid body (Paik, *et al.*, 1996).

Costas, *et al*., 2003 studied the influence of fulfillment of crash boxes with different materials. They performed both quasi-static and dynamic experimental tests. The results were compared with numerical simulations using finite element method (FEM). These authors also presented parameters used to evaluate the crashworthiness of the specimens. Such parameters are:

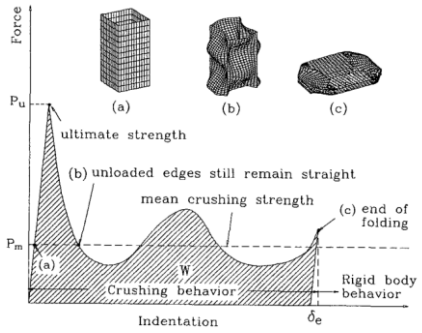

Figure 1 – Crushing behavior of a square tube under compressive loads (Paik, *et al*., 1996)

Absorbed Energy (E_a): calculated as the area under the Load-Displacement Curve:

$$E_a = \int_0^{\delta} F(z)dz \tag{1}$$

where $F(z)$ is the axial force and δ is the total displacement.

Specific Energy Absorption (*SEA*): this parameter is a very important efficiency indicatior of the energy absorber, specially when a weight reduction is desired. It is the ratio between the absorbed energy and the mass (m) of the specimen:

$$SEA = \frac{E_a}{m} \tag{2}$$

Mean Crushing Load (P_m): The mean of the applied force. It can be calculated as the ratio of the absorbed energy and the total displacement:

$$P_m = \frac{E_a}{\delta} \tag{3}$$

Load Ratio (*LR*): this value should be as low as possible in order to reduce the acceleration felt by car occupants. It is calculated as the ratio between the initial peak load (P_{peak}) and the mean load:

$$LR = \frac{P_{peak}}{P_m} \tag{4}$$

Nakazawa, *et al*., 2005 performed experimental tests and numerical simulations using specimens with various cross sections to obtain an optimized section for automotive crash box (see Fig. 2). According to these authors, their work can change the design of automotive parts for crash energy absorption and can contribute to the weight reduction of steel parts, since the cross section proposed by them absorbed twice impact energy when compared to conventional design.

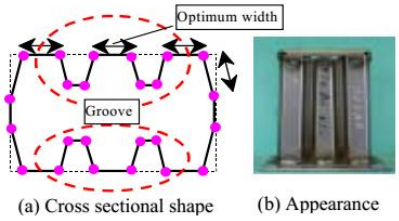

Figure 2. Cross section developed by Nakazawa, *et al*., 2005

Considering the works treated at this paper, two of them were of main importance (Tarigopula *et al.*, 2006, Kazanci and Bathe, 2012). Then, at this paper the dimensions of the reference sample is the same shown at those works after

some changes are done as it will be described at section 2. Tarigopula, *et al*., 2006 have studied the behaviour of tubes loaded under quasi-static and dynamic compression loads. They studied the energy absorption capability of tubes with square and top hat sections. The tubes were made with a high strength-steel alloy called DP800. Authors obtained the load-deformation history of the specimens, as shown in Fig. 3 for a square tube and calculated the energy absorbed as the area under this curve. The work mentioned in this paragraph provides a valuable contribution on the efficiency of energy absorbers since it provides numerical and experimental results. For that reason, the results from Tarigopula *et al*., 2006 are used in present study as reference. As described later in section 2, the simulations performed in the present work were run using a similar approach used by Tarigopula *et al*., 2006.

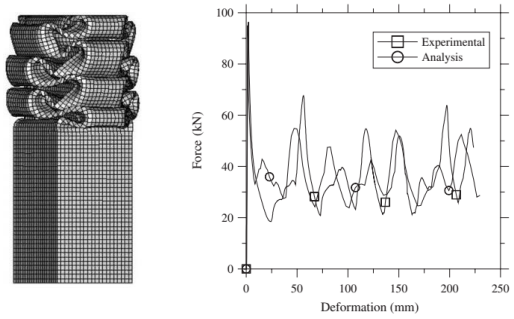

(a) (b)

Figure 3. Results of quasi-static studies of a square section specimen (a) collapsing profile from simulations; (b) load -displacement history. (Tarigopula, *et al.*, 2006)

Kazanci and Bathe (2012) used the numerical and experimental data published by Tarigopula, *et al.*, 2006 in order to investigate the use of implicit time integration techniques to solve crushing and crashing problems. It is mentioned by the authors that for crush and crash simulations the explicit time integration is generally used. The explicit time integration is suitable for simulations that requires small time steps to investigate the dynamic response and to simulate the events where the maximum response occurs in a short time interval, while the implicit time integration can be ideally used for solving problems with a long time duration. Even in the cases that the implicit integration is more suitable, the explicit time integration is widely used due the fact that the convergence in implicit integration is more difficult to be achieved (Kazanci and Bathe, 2012). In this sense, the authors proposed the use of implicit time integration to solve the problem described by Tarigopula *et al.*, 2006. They achieved a very good agreement between their results and the results published by Tarigopula *et al.*, 2006.

Some recent works investigate the presence of windows on the lateral faces of the tubes. Song *et al*., 2013 performed crush analysis of tubes with rectangular windows. They executed parametric analysis using FEM by varying the windows size (dimensions "a" and "b" in Fig. 4c). Their results showed an increase in the specific energy absorption and a decrease in the peak load. Auersvaldt (2014) also used a parametric study using FEM in order to investigate the influence of the windows dimensions on the energy absorption indicators. Auersvaldt (2014) also varied the shape of the cross section of the tubes. He simulated square, hexagonal, and double hat tubes. As noted by Song *et al.*, 2013, Auersvaldt (2014) also verified a decrease at the peak load when windows were placed on the lateral faces of the specimens.

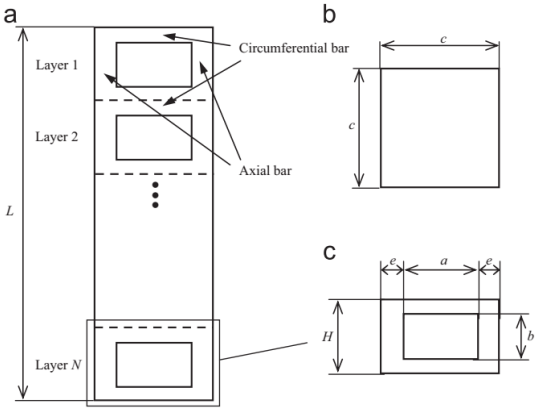

Figure 4. Representation of a widowed tube: (a) side view, (b) top view, and (c) side view of one layer. (Song *et al.*, 2013)

The literature concerning the study of energy absorbers shows the importance of numerical simulations in such analysis. Thus, the present work aims to evaluate the efficiency of square tubes as energy absorbers when axially compressed. Some simulations using a commercial FEM software were performed and the influence of parameters such as specimen dimensions and mechanical properties of the material are studied. The analysis of the results showed variation on the energy absorbed, specific energy absorption, mean crushing load and also on the load ratio when the wall thickness and material were changed.

2. METHODOLOGY

Numerical simulations using a commercial package were performed in order to evaluate the influence of changing the wall thickness of the tubes and the material properties. A combination of three materials and two wall thickness (t) were studied in a total of six simulations, as shown in Tab. 1. Each simulation was named in the format XX_Y.YY, where XX stands for the material (DP means DP800, ST means steel, and AL means aluminum) and Y.YY is the wall thickness in millimeters. DP800 is a high strength steel alloy, and its properties were studied by Tarigopula *et. al*., 2006.

Table 1. Simulations Summary

Simulation Identification	Material	Wall Thickness t (mm)
DP_1.18	DP800	1.18
DP_1.50	DP800	1.50
ST_1.18	Steel	1.18
ST_1.50	Steel	1.50
AL_1.18	Aluminum	1.18
AL_1.50	Aluminum	1.50

Dimensions of the tubes were obtained from the works of Tarigopula, *et al*., 2006 in order to allow a comparison between the numerical results from the present study and the results presented by the referenced authors. For that reason, the specimens simulated have square cross sections with width of 60 mm (measured in the centerline of the sheet) and are 410 mm in length, as shown in Fig. 6. The wall thickness of the tubes is a variable of study and is shown in Tab. 1 for each simulation.

The materials were chosen considering the possibility of use in automotive applications and its availability for fabrication of physical specimens, in order to perform experimental analysis in future studies. As described below, tension tests were performed in steel and aluminum sheet specimens in order to get the mechanical properties of the materials used in simulations. The metal sheets used to fabricate the specimens were bought in a commercial store, where it was told that the steel is a low carbon steel (SAE 1010) and the aluminum is common aluminum.

The mechanical properties of DP800 were obtained from the work of Tarigopula, *et al.*, 2006, while the properties of Steel and Aluminum were obtained by performing tension tests according to the standard ASTM E8M. Some properties, such as density and Poisson's Ratio were obtained from the literature due the difficult to obtain those properties experimentally. The mechanical properties used in the simulation are shown in Tab. 2, where E means Young's Modulus, v means Poisson's Ratio, σ_y means yield strength, E_t means Tangent Modulus, and γ means density.

Two plasticity models were tested: Multilinear Isotropic Hardening and Bilinear Isotropic Hardening according to the commercial package used. The difference between these two models is that the Bilinear Isotropic Hardening represents the plastic portion of the Stress Strain Diagram with a single line with inclination E_t (tangent modulus), while the Multilinear Isotropic Hardening uses points of Trues Stress vs True Plastic Strain to model the behavior of the material in the plastic zone. These two models are illustrated in Fig. 5.

In the Bilinear Isotropic Hardening, the tangent modulus varies with strain, which means that there is no single value for this property. In this work, the Bilinear Isotropic Hardening was used to perform only the simulations of the material DP800, due the availability of the results from Tarigopula, *et al.*, 2006. The experimental data presented from these authors, were very useful to calibrate the model, since it was used to verify which valor of E_t best represents the material DP800. In this sense, a convergence study was done in order to figure out what value of E_t best fit the experimental results. The value of E_t = 6561 MPa was chosen because this value lead to an error less than 7% when the absorbed energy calculated using data from simulations were compared with the experimental results from reference work.

For Steel and Aluminum, the Multilinear Isotropic Hardening Model was adopted since there are no experimental data for the specific crushing conditions of the problem studied, so a convergence analysis of E_t was not viable.

A description of the simulations is presented in the next section, where some simulations parameters such as mesh and solution type are described.

Table 2. Mechanical Properties Used in Simulations

Material	**Mechanical Property**				
	E (GPa)	ν	σ_y (MPa)	E_t (MPa)	γ (kg/m^3)
DP 800	195[(1)]	0.33[(1)]	495[(1)]	6561[(2)]	7850[(1)]
Aço	195[(3)]	0.30[(4)]	172[(3)]	-	7850[(4)]
Alumínio	63[(3)]	0.33[(4)]	112[(3)]	-	2700[(4)]

[(1)]From Tarigopula, *et al*., 2006
[(2)]Calculated using data published by Tarigopula, *et al*., 2006
[(3)]From Tensile Tests performed by the authors
[(4)]From Callister, 2007

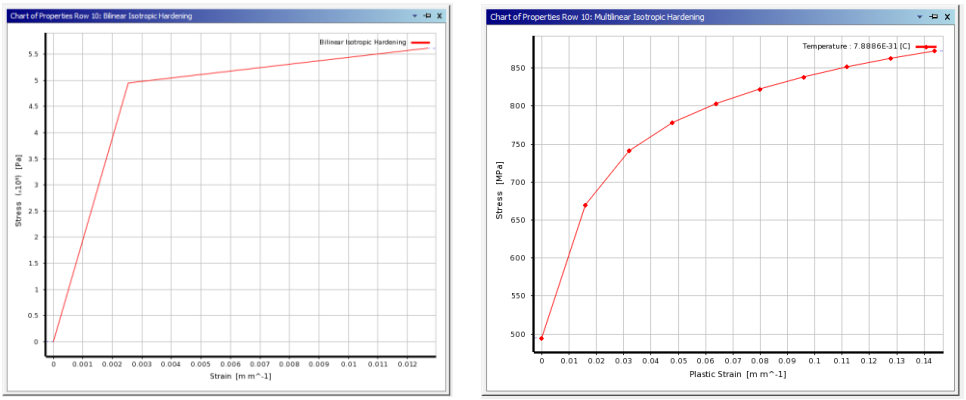

(a) (b)

Figure 5. Plasticity Models Used in Simulations: (a) Bilinear Isotropic Hardening (elastic and plastic region) and (b) Multilinear Isotropic Hardening (only plastic region)

2.1 Simulations Description

The simulations were carried out using Explicit Dynamics Analysis. As stated before, the procedures of Tarigopula, *et al.*, 2006 were reproduced in order to allow results comparison. Thus, the tube were crushed between two solid plates by the movement of the upper plate (see Fig. 6c). A velocity was imposed to the upper plate. The interaction of the three bodies were considered as frictional and a friction coefficient equal to 0.3 was used.

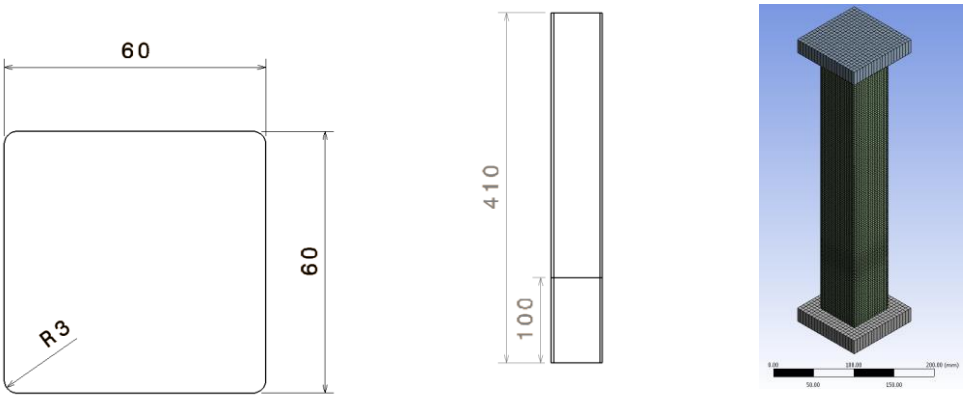

(a) (b) (c)

Figure 6. (a) Cross-Section Dimensions, (b) Length of the tube and (c) Isometric view of tube and crushing plates

The geometry were created using an external CAD software and then imported to the FEM commercial package. Some geometric imperfections were introduced on the side walls of the tubes in order to account the out-of-flatness of the wall. The imperfection were introduced as a half sine wave with amplitude of 0.05 mm, as shown in Fig. 7. A radius of 3 mm (not shown in Fig. 7) rounded corners of the tube, as done in the reference work.

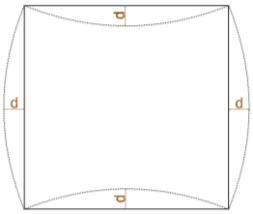

Figure 7. Geometric Imperfections of Tube's Cross section (d = 0.05 mm was used in simulations)

For the tube, the element size was 3mm x 3mm, which generates a total of 12852 elements and 12936 nodes. At the corners, three elements were placed across the arcs. The simulations were performed using quadrilateral linear shell elements (quad4). For the plates, the size of the elements was chosen as 5 mm, which gave a total of 400 elements and 441 nodes for each plate. The elements used in plates were also quadrilateral linear shell elements. As a mesh metric, the element quality was chosen. The minimum value obtained for element quality was 0.71179 and the maximum value was 0.99947, which means the mesh presents a good quality since the maximum quality element is 1.

All degrees of freedom of the tube's bottom line were restrained by a fixed support in order to fix the tube, and all the rotational degrees of freedom of the elements at the upper end were restricted in order to avoid numerical problems due possible unrealistic deformation. Also, the displacements in lateral directions of the lower 100 mm portion of the tube were constrained. In that portion, only the longitudinal displacement was set free in order to allow axial deformation. This constraint method were used to simulate the experimental set up, since the lower 100 mm of the specimens was clamped during the crushing process. Another reason to use this constraint method is the fact that experimental tests with these constrains are going to be performed in the future.

The velocity imposed in the upper plate was ramped from 0 m/s to 6.33 m/s in a time interval of 25 ms. Then the velocity was kept constant until the end time of the simulation (50 ms). According to Tarigopula, *et al.*, 2006, this approach ensures that the kinetic energy is insignificant when compared to the strain energy absorbed by the crushing of the specimen. Figure 8 shows the velocity profile used in the simulations.

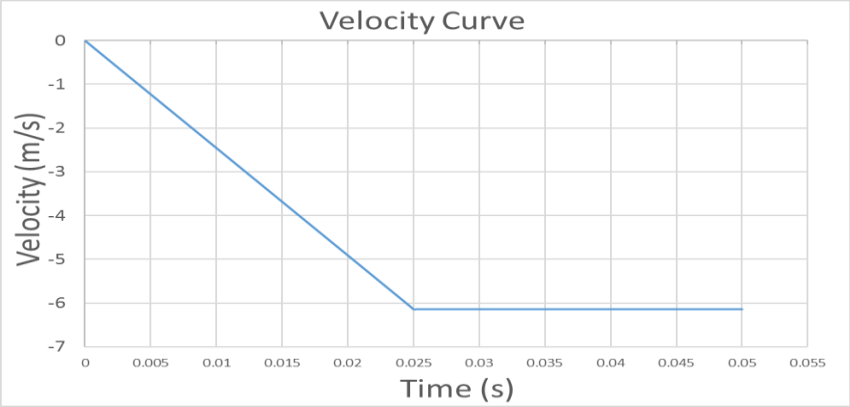

Figure 8. Velocity profile used in simulations. Negative values mean the velocity was applied in negative direction of the coordinate system.

In all simulations, the load displacement history was obtained. This curve is the most important output of the simulation, because it is necessary to calculate the absorbed energy. The data points (displacement and axial force) acquired in simulations were recorded and analyzed using the software Matlab®. The absorbed energy was calculated using the area under the Load-Displacement curve.

3. RESULTS

Table 3 presents the results obtained in the six simulations and the results of reference work. The simulation identifier (column 1 in Tab. 3) is explained in section 2 (see Tab. 1).

The following part of this section is divided in three subsections: comparison between present study and the reference work (results from Tarigopula, *et al., 2006.*), influence of wall thickness variation, and influence of material change. In all subsections, the load displacement curve and the collapsible modes of the specimens are presented.

Table 3 – Results Summary

	Absorbed Energy (kJ)	**Mass (kg)**	**Specific Energy Absorption (kJ/kg)**	**Mean Crushing Load (kN)**	**Peak Load (kN)**	**Load Ratio P_{peak}/P_m**
Reference work [(1)]	8.08	-	-	36.2	96.3	2.66
DP_1.18	8.64	0.892	9.69	37.6	137	3.64
DP_1.50	14.3	1.13	12.6	62.3	177	2.84
ST_1.18	2.82	0.892	3.16	12.3	51.7	4.21
ST_1.50	4.36	1.13	3.84	18.9	67.2	3.55
AL_1.18	1.30	0.307	4.25	5.66	30.7	5.42
AL_1.50	2.06	0.390	5.29	8.97	39.6	4.41

[(1)]Experimental results from Tarigopula, *et al*., 2006. Material is DP800 and wall thickness is 1.18 mm.

3.1 Comparison between present study and the reference work

In order to validate the simulations performed in this work, comparisons between the results obtained here and the reference work were made. For that reason, the simulation DP_1.18 was carried out using a specimen with the same dimensions and mechanical properties used by Tarigopula, *et al*., 2006.The numerical results obtained in this work show an acceptable agreement with the results presented by the reference authors, as can be seen in Tab. 3 and Fig. 9. The absorbed energy presented an error of approximately 7% when compared to the experimental results. The mean crushing load error was less than 4%. The parameter that present a significant error was the peak load (an error about 42%). This discrepancy can be occasioned by numerical instability and further investigations have to be done in order to evaluate the cause of this excessive value of peak load. It is important to state that the software used at present work is not the same software used by Tarigopula *et al.*, 2006.

The shape of the collapse specimen (Fig. 9d) presents a good agreement with the collapse profile shown in reference work (Fig. 9b and Fig. 9c). All three specimens formed the same number of lobules, as can be seen in Fig. 9.

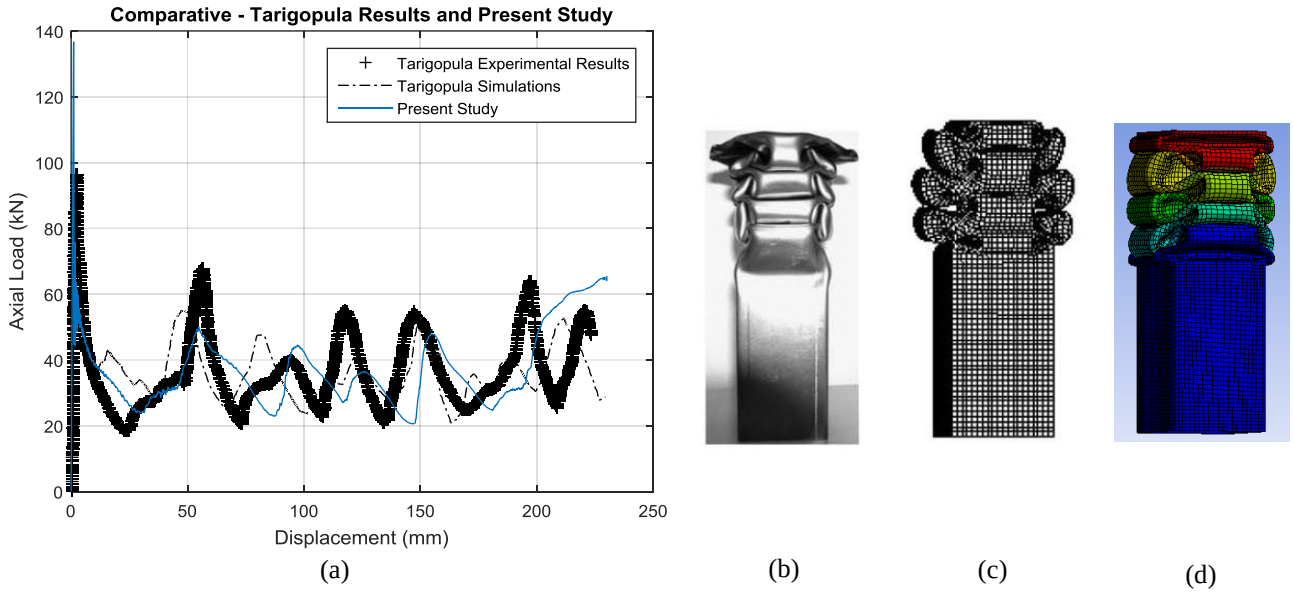

Figure 9. Comparative of present study and reference work. (a) Load-Displacement Curves, (b) experimental collapse profile from reference work, (c) numerical collapse profile from reference work, and (d) collapse profile from present study

3.2 Influence of wall thickness variation

The results showed an increment in the axial load when the wall thickness of the tube was increased. This phenomenon can be noted by the examination of Load Displacement Curves shown in Fig. 10a, Fig. 11a, and Fig. 12a. For the same material, the shape of the curves was similar and the magnitude of the axial force is the most notable change.

The collapse profile of steel and aluminum tubes did not present important differences; the main difference was in DP800, which can be verified by comparing Fig. 10b with Fig. 10c. Also, the final end of the Load Displacement curve obtained in simulation DP_1.50 shows a shape difference when compared to the curve generated from simulation DP_1.18, as can be seen in Fig. 10a. According to Fig.10c, the first lobule has its ends facing the top and the others fold in the opposite direction. As the stiffness of the tube is greater at the end, the set of lobules seems to give more rigidity and a peak of force happens. At the curve with t = 1.50 mm the second peak is disturbed by the first (opposite sense), by the way the peak is smaller than the first. The third restore the force and the forth shows a gain. The peaks of force, excepting the first, at the curve t = 1.18 mm are more uniform.

When comparing the values obtained for DP800, the absorbed energy increased 5.66 kJ when the thickness was increased, which corresponds to a difference of 66%. The Specific Energy Absorption increased 2.91 kJ/kg (30% of increment), and the mean crushing load increased 66%. The load ratio decreased from 3.64 to 2.84. As stated in the introduction of this paper, the load ratio has to be as low as possible to reduce the acceleration felt by passengers. Therefore, a decrease in this value is an improvement for the energy absorption process.

For steel simulations, when the wall thickness was increased from 1.18 mm to 1.50 mm the absorbed energy increased 1.54 kJ (about 55%), the Specific Energy Absorption increased 0.68 kJ/kg (22%) and the mean crushing load increased 6.6 kN (about 54%). The load ratio decreased 16%, which means the increment in wall thickness contributes positively.

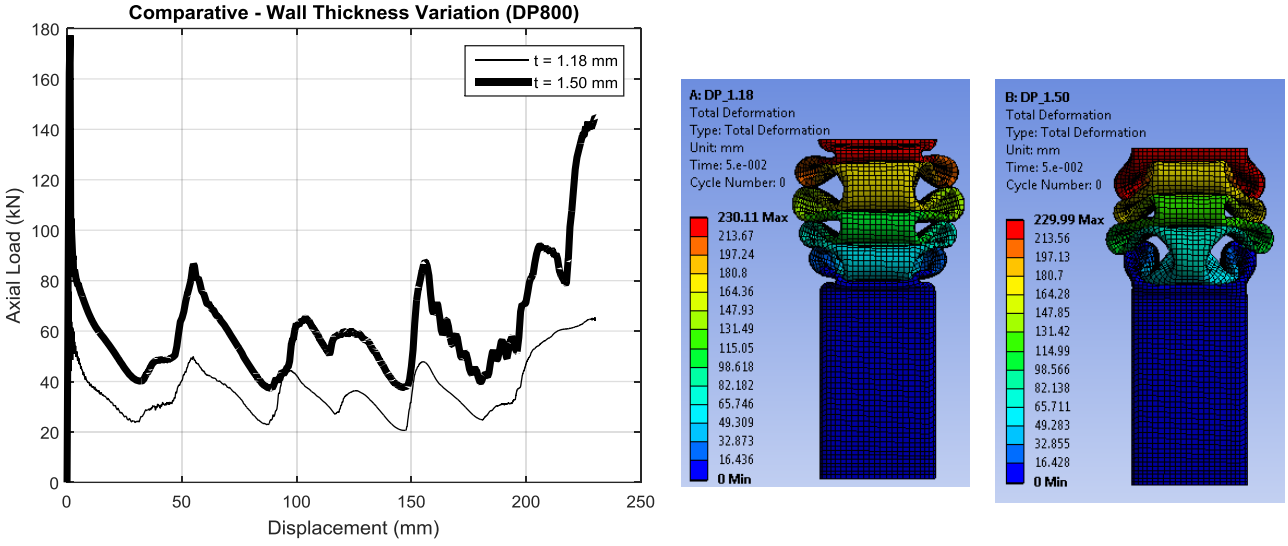

(a) (b) (c)

Figure 10. Effects of wall thickness variation in Load Displacement History and Collapsing mode for DP800. (a) Load-Displacement Curves, (b) collapse profile for t = 1.18 mm, and (c) collapse profile for t = 1.50 mm

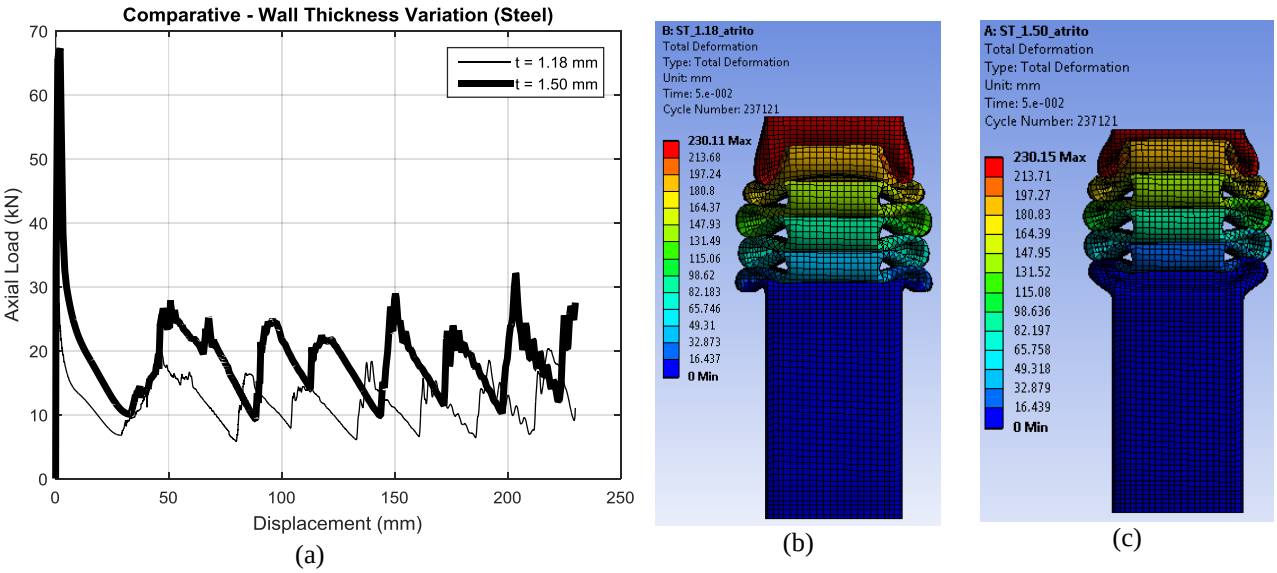

(a) (b) (c)

Figure 11. Effects of wall thickness variation in Load Displacement History and Collapsing mode for Steel. (a) Load-Displacement Curves, (b) collapse profile for t = 1.18 mm, and (c) collapse profile for t = 1.50 mm

In the simulations using aluminum, similar results were obtained. When the wall thickness was increased from 1.18 mm to 1.50 mm the absorbed energy increased from 1.30 kJ to 2.06 kJ (58%), while the Specific Energy Absorption increased 1.04 kJ/kg (24%). The mean crushing load increased 3.3 kN (58%) and the load ratio decreased from 5.42 to 4.41 (about 19%).

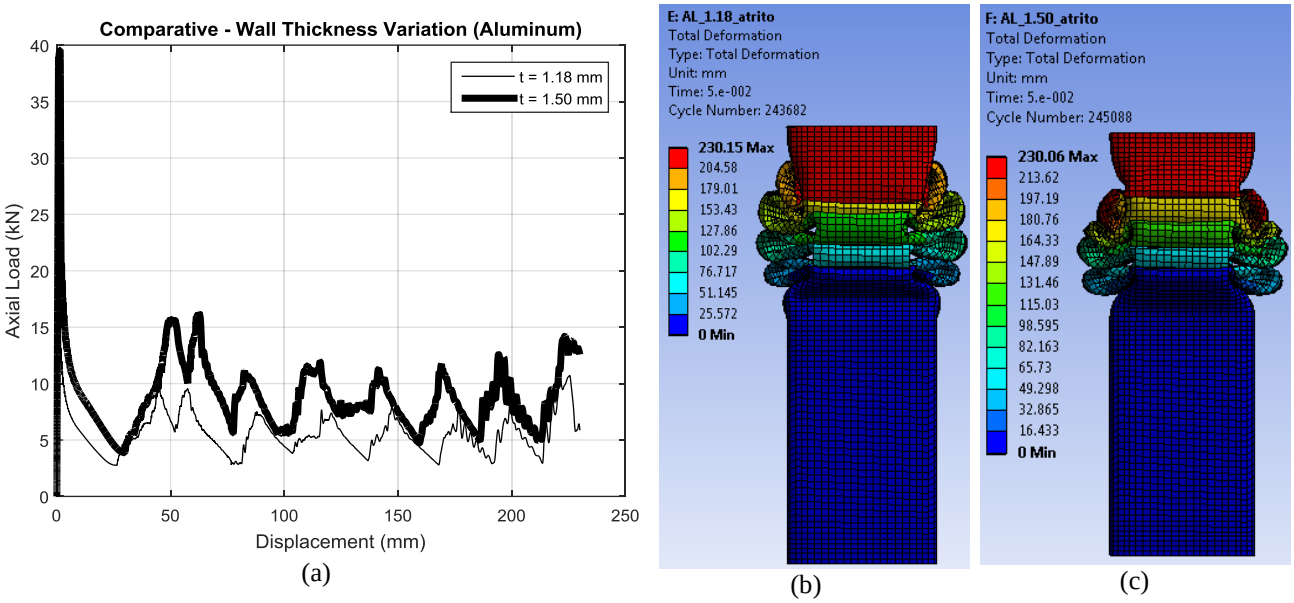

(a) (b) (c)

Figure 12. Effects of wall thickness variation in Load Displacement History and Collapsing mode for Aluminum. (a) Load-Displacement Curves, (b) collapse profile for t = 1.18 mm, and (c) collapse profile for t = 1.50 mm

3.3 Influence of material change

Figure 13 and Figure 14 show the influence of material change in the Load Displacement Curve. The modification in the shapes of the curves denotes the difference in collapse profiles. This differences can be checked by comparison of Fig. 10b, Fig. 11b, and Fig. 12b for specimens having t = 1.18 mm and Fig. 10c, Fig. 11c, and Fig. 12c for specimens having t = 1.50 mm.

The magnitudes of the changes can be verified in Tab. 3. This table shows the material which absorbs the greatest amount of energy is DP800, followed by steel and aluminum. Considering the Specific Energy Absorption, aluminum presented a better performance than steel, since aluminum presented a SEA value 34% higher than steel for t = 1.18 mm and 38% higher than steel for t = 1.50 mm.

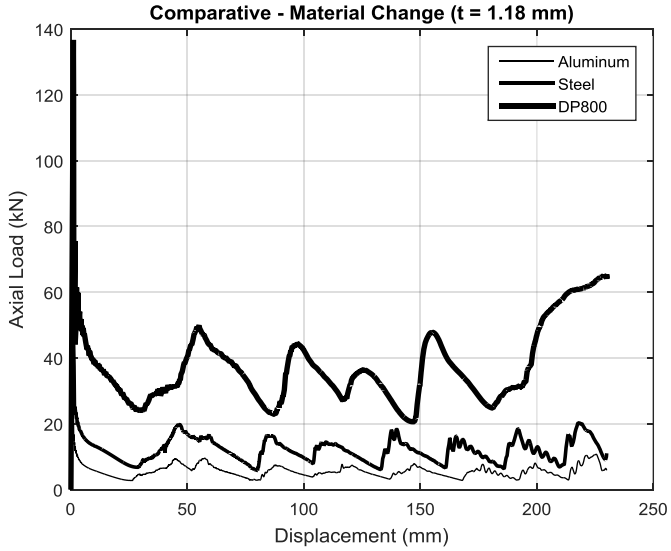

Figure 13. Effects of material changing in Load Displacement History using wall thickness of 1.18 mm

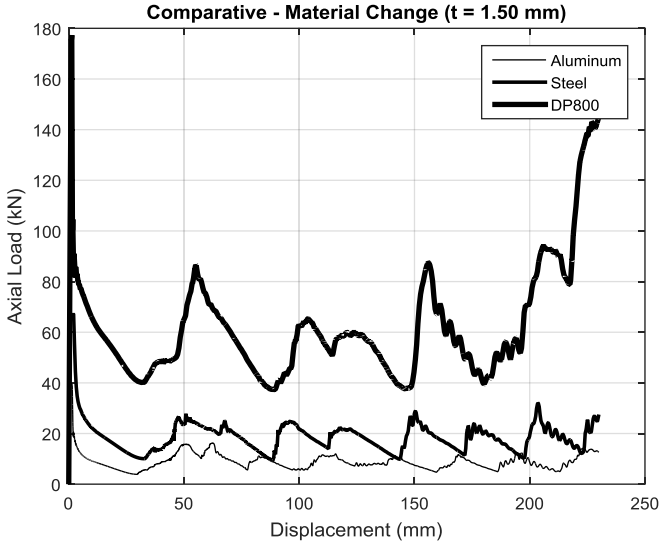

Figure 14. Effects of material changing in Load Displacement History using wall thickness of 1.50 mm

4. CONCLUSIONS

The review of the literature denotes the importance of simulations when analyzing the efficiency of energy absorbers. By performing numerical simulations, the influence in materials change and wall thickness variation were analyzed. The results shown that the absorbed energy increases significantly with the wall thickness increment. Also, the mechanical properties of material used in simulations have an important role in the performance of energy absorbers.

The use of the FEM commercial package used to carry out the study on crushing shell structures seems to be suitable because it considers non-linear behavior of the structure during crushing events. At these events energy absorbed, specific energy absorbing, mean crushing force, and load ratio seem to be of great importance to evaluate crash boxes performance.

5. ACKNOWLEDGEMENTS

The authors would like to thank DENATRAN – Departamento Nacional de Trânsito for some financial support of this project. We also would like to thank FAPDF – Fundação de Apoio à Pesquisa do Distrito Federal for paying the costs of participation in the event in which this paper is going to be presented.

6. REFERENCES

Auersvaldt, R.R., 2014. *Análise paramétrica de absorvedores de energia de impacto poligonais com janelas laterais*. Dissertation, University of São Paulo, São Paulo, Brazil.

Callister, W.D.J., 2007. *Materials Science and Engineering – An Introdution.* John Wiley & Sons, York, PA, 7th Edition.

Costas, M., Díaz, J., Romera, L.E., Hernandéz, S., & Tielas, A., 2013. "Static and dynamic axial crushing analysis of car frontal impact hybrid absorbers". *International Journal of Impact Engineering*, vol. 62, pp. 166-181.

Kazanci, Z. and Bathe, K.J., 2012. "Crushing and crashing of tubes with implicit time integration". *International Journal of Impact Engineering*, vol. 42, pp 80-88.

Nakazawa, Y., Tamura, K., Yoshida, Takagi, K., Kano, M., 2005. "Development of crash box for passenger car with high capability for energy absorption". *VIII International Conference on Computational Plasticity*, Barcelona, Spain.

Paik, J. K., Chung, J. Y., Chun, M. S., 1996. "On Quasi-Static Crushing of a Stiffened Square Tube". *Journal od Ship Research*, vol.40, n.3, pp. 258-267.

Song J., Chen Y. and Lu, G., 2013. "Light-weight thin-walled structures with patterned windows under axial crushing". *International Journal of Mechanical Sciences*, vol. 66, pp. 239-248.

Tarigopula, V., Langseth, M., Hopperstad, O.S., & Clausen, A.H., 2006. "Axial crushing of thin-walled high-strength steel sections". *International Journal of Impact Engineering*, vol. 32, n. 5, pp. 847-882.

7. RESPONSIBILITY NOTICE

The authors are the only responsible for the printed material included in this paper.